LUNDS
UNIVERSITET

DEPARTMENT of PSYCHOLOGY

Resting-state Functional Connectivity in Anhedonia: Exploring the Effects of Pramipexole

Frida Smids

Master's Thesis (30 hp)
Spring 2023

Supervisor: Johannes Björkstrand

Abstract

Pramipexole is a medication that normalises dopamine signalling in the brain. Previous studies have suggested that pramipexole is an effective treatment option for depression and anhedonia because it targets the dopaminergic pathways within the brain's reward network. The nucleus accumbens is a crucial region for dopamine signalling in reward processing. Both task-based and resting-state fMRI evidence have supported the association between anhedonia and abnormal connectivity of the nucleus accumbens. However, no previous research has directly compared how the nucleus accumbens resting-state functional connectivity is altered pre-and post-pramipexole treatment.

This study analysed resting-state fMRI data that was collected before and after treatment with pramipexole in a sample of patients with depression and anhedonia (N=9). Bilateral nucleus accumbens seeds were correlated with all other voxels in the brain in a seed-to-voxel functional connectivity analysis. A general linear model was conducted to average the seed-based connectivity maps for main effects of the pre-and post-treatment sessions respectively, and to compare connectivity between the two sessions.

Significant differences in resting state functional connectivity of the bilateral nucleus accumbens was found in two regions: the left intracalcarine cortex and the right lingual gyrus. In both regions, resting state functional connectivity had switched from positive pre-treatment to negative post-treatment. The present findings are interpreted taking the study's limitations into account, and suggestions are made for future research.

Keywords: *Anhedonia, Depression, Reward, Pramipexole, Resting-state, Functional Connectivity, Nucleus Accumbens*

Introduction

Anhedonia is the lack of, or decreased ability to, experience pleasure and recollect joyful experiences. Patients with anhedonia may show less interest in things or not engage in activities they used to enjoy (American Psychiatric Association, 2013). Anhedonia can be a feature of several different psychopathologies; however, it has been found to be most severe in major depressive disorder (MDD) (Trøstheim et al., 2020). When comorbid with depression, anhedonia has been found to predict worsened illness progression (Spijker et al., 2010; Vrieze et al., 2013). For example, Auerbach et al. (2015) compared suicidal adolescents and found that suicide attempters reported more severe anhedonia than suicide ideators. In turn, anhedonia does not respond as well to serotonin reuptake inhibitors, which are often prescribed as antidepressants (McMakin et al., 2012).

The last two decades have seen an increase in research on the neurobiological processes of anhedonia, but there remain gaps in the literature (Pizzagalli, 2022). By understanding the cognitive processes and neurobiology of anhedonia, patients at high risk of worsened illness progression can be identified, and effective treatment options can be developed (Wacker et al., 2009). The current study aims to explore how resting-state functional connectivity is altered in patients with depression and anhedonia after treatment with pramipexole, a dopamine agonist.

The Cognitive and Neurobiological Processes of Anhedonia

Anhedonia is associated with abnormalities or deficits in reward processing (Borsini et al., 2020; Zhang et al., 2016). Processing rewards can be broken down into distinct phases: (1) recognising that something is a reward, (2) calculating the value of that reward, (3) calculating the effort of going after the reward, (4) deciding to do so, and (5) anticipating a reward and being motivated by it (Der-Avakian & Markou, 2012). In the context of functional neuroimaging research, the monetary incentive delay task (MID) and the probabilistic reward task (PRT) are standard tools used to activate reward processing in the brain. The MID task has three elements: anticipation, target, and feedback, and it can target both reward and loss processing (Knutson et al., 2000; Wilson et al., 2018). The PRT is a signal-detection task that assesses hedonic capacity, i.e., change in behaviour as a response to a reward (Pizzagalli et al., 2005). Using the PRT, Pizzagalli et al. (2005) found that among healthy participants, those who scored higher on a depressive symptomatology scale showed reduced reward responsiveness than those who scored lower. Furthermore, they found that participants with higher scores on anhedonia and melancholic scales were less likely to develop response bias throughout the task

(i.e., they were less likely to modulate their behaviour based on previous reinforcement of that stimuli).

Neuropsychology research often uses the PRT or MID, among other tasks, to activate the brain regions involved in reward processing during brain imaging. One brain imaging tool is functional magnetic resonance imaging (fMRI). fMRI measures blood oxygen level-dependent (BOLD) signals in the brain. As neurons activate, the hemodynamics of that region change and fMRI captures how the concentration of deoxygenated and oxygenated blood changes as a result of neuronal activity (Jenkinson & Chappell, 2018; Ogawa et al., 1990). fMRI is limited to implying neuronal activity, since the method cannot measure neurons' electrochemical activity directly. Nevertheless, there are several research opportunities using this technique. For example, to compare how brain activity in a specific area changes across task conditions or between groups. Research using fMRI has found that reward and motivation processing occur along the mesocortical and mesolimbic pathways that span across hubs in the brain associated with cognitive control, emotion, and learning processes (Hauser et al., 2017; Heshmati & Russo, 2015). Knutson et al. (2000) found early fMRI evidence that the MID task activates the striatal and mesial prefrontal circuitry. They discovered that rewards activate the caudate, putamen, medial prefrontal cortex, and left motor cortex. Further studies have found activation in the striatum and within the putative salience network, including the anterior cingulate cortex, when anticipating rewards and losses (for meta-analysis, see Wilson et al., 2018).

Anhedonia is not a deficiency in all five reward processes but is associated with abnormal consummatory (i.e., liking), and anticipatory (i.e., wanting) processing, as well as reward learning (Borsini et al., 2020; Pizzagalli, 2022). During these phases of a reward task, patients with depression and anhedonia have shown reduced activity in the ventral striatum, ventral tegmental area, caudate and putamen (Borsini et al., 2020; Zhang et al., 2016), as well as the perigenual and dorsal anterior cingulate cortex (Pizzagalli, 2022). Reduced activity in the orbitofrontal cortex has also been identified (Xie et al., 2021). A recent meta-analysis by Borsini et al. (2020) summarised the literature and found that the neurobiological processes, as they related to anhedonia, did overlap but remained distinct for the different reward processes. The authors found that the consummatory phase was distinctly associated with less activation in the right anterior insula. During the anticipatory phase of reward tasks, there was evidence of hypo- and hyperactivation in the frontal cortex in patients with anhedonia. Lastly, some evidence indicated that deficits in reward learning in participants with anhedonia were associated with

less activity in the striatum, ventromedial prefrontal cortex, anterior cingulate cortex and orbitofrontal cortex (Borsini et al., 2020).

Dopamine and the Nucleus Accumbens

Reward processing involves different neurotransmitters. Dopamine has been considered a key neurotransmitter, but the role of opioid, glutamatergic, and serotonergic systems have also been recognised in the literature (Höflich et al., 2019). It has been suggested that different neurotransmitters are related to different phases of reward processing (Der-Avikan & Markou, 2012; Höflich et al., 2019). For example, early evidence from participants with pathological obesity found that dopamine is associated with reward anticipation and motivation (Wang et al., 2002). Borsini et al. (2020) proposed that neurochemical signalling separates reward learning, anticipatory, and consummatory processes. They suggested that anticipatory processing and reward learning is associated with dopamine signalling, whilst consummatory processing is associated with opioid signalling.

The current study will focus on the role of dopamine. Dopamine signalling occurs within different pathways in the brain. The mesolimbic pathway has cell bodies in the VTA and substantia nigra and projects to the ventral striatum, limbic regions, and amygdala (Dunlop & Nemeroff, 2007). The prefrontal cortex has also been associated with this pathway (Heshmati & Russo, 2015). The mesolimbic pathway is associated with emotional regulation, reinforcement learning, and hedonic capacity (Dunlop & Nemeroff, 2007). In contrast, neurons in the mesocortical pathway also have their cell bodies in the VTA and substantia nigra but project to the anterior cingulate cortex, orbitofrontal cortex, and the prefrontal cortex; this pathway is associated with processing reward effort (Hauser et al., 2017), as well as concentration and executive functions (Dunlop & Nemeroff, 2007).

Both the mesocortical and mesolimbic pathways are essential for the experience of pleasure and are both relevant to understanding the neurobiological deficits in anhedonia (Der-Avakian & Markou, 2012). The current study focused on the mesolimbic pathway and the nucleus accumbens (NAc) in the ventral striatum as it is more consistently referred to as a reward processing pathway (Dunlop & Nemeroff, 2007; Höflich et al., 2019). The ventral striatum is part of the limbic system. In addition to the NAc, the ventral striatum comprises the olfactory tubercle and parts of the caudate and putamen. The NAc receives dopaminergic, serotonergic, histaminergic and glutamatergic projections (Ding et al., 2022; Russo & Nestler, 2013; Yager et al., 2015). As part of the mesolimbic pathway the NAc receives dopaminergic projections from the ventral tegmental area. The function of this circuitry is recognition of

rewards and initiating behaviour towards the reward (Jonasson et al., 2014; Nestler & Carlezon, 2006), as well as reward motivation and learning (Treadway & Zald, 2011). It has been suggested that the deficits in the VTA-NAc dopamine circuitry plays a vital role in the pathophysiology of anhedonia (Nestler & Carlezon, 2006). Furthermore, anhedonia has been found to be associated with reduced NAc volume (Auerbach et al., 2017; Wacker et al., 2009) and weaker NAc response during reward tasks (Borsini et al., 2020; Pizzagalli et al., 2009; Pizzagalli, 2022; Wacker et al., 2009), including during both consummatory and anticipatory phases of the tasks (Borsini et al., 2020).

In light of the central role of dopamine in reward processing, there have been attempts at treating anhedonia with dopaminergic medication (Höflich et al., 2019). For example, Admon et al. (2017) conducted a double-blind, randomised, placebo-controlled study with amisulpride with unmedicated participants with depression and healthy controls. Participants received a single dosage of amisulpride or placebo and completed the MID as well as the PRT. The study found that the participants who received the amisulpride showed increased striatal activity when responding to rewards during the MID, compared to the placebo group. They also found increased corticostriatal functional connectivity during the task, including between the NAc and the midcingulate cortex in the depressed group who received amisulpride; this was related to better reward learning (Admon et al., 2017). These results indicate not only that striatal activity and functional connectivity with the NAc are related to deficient reward processing in depression but also that acute dopaminergic medication can be a successful pharmacological treatment for anhedonia.

Pramipexole

Like amisulpride, pramipexole is a dopamine agonist. A dopamine agonist activates dopamine receptors in the postsynaptic neuron, thereby mimicking the effect of endogenous dopamine release. In this way, pramipexole normalises dopamine signalling (Chernoloz et al., 2009). Pramipexole also has neuroprotective (i.e., preventing neuronal death) and neurorestorative effects (i.e., restoring neuronal damage) (Fawcett et al., 2016; Joyce & Millan, 2007). Pramipexole has primarily been used to treat Parkinson's disease, where deficient dopaminergic signalling is known to be a central part of the pathophysiology (Antonini et al., 2010; Jiang et al., 2021) but has also been shown to affect depression. Two recent meta-analyses of randomised controlled trials of pramipexole in patients with Parkinson's disease found supporting evidence for the efficacy of pramipexole in both symptoms of Parkinson's disease and depression (Jiang et al., 2021), as well as quality of life (Li et al., 2022). Furthermore,

pramipexole has been shown to affect depression without Parkinson's disease (for review and meta-analysis, see Tundo et al., 2019).

Pramipexole has a high affinity for the D2 subfamily of dopamine receptors (Antonini et al., 2010; Chernoloz et al., 2009; Hubble, 2000), in particular, D3 receptors. For example, a study by Maj et al. (2000) found that pramipexole injections in rats would increase D3 responsiveness. They also found increased D3 receptor binding in regions of the ventral striatum. D3 receptors can be found in the NAc have been associated with reward, motivation, and emotional processing in drug addiction (Heidbreder et al., 2005; Hubble, 2000; Sokoloff & Le Foll, 2017). Thus, we can hypothesise that pramipexole, due to its affinity for D3 receptors, would be an effective treatment for depression and anhedonia (Leggio et al., 2013).

A recent study by Ventorp et al. (2022) compared BOLD-response during a monetary incentive delay task before and after a 10-week pramipexole treatment in a patient sample with depression and anhedonia. They found preliminary evidence suggesting that depression and anhedonia symptoms were reduced after treatment. When comparing BOLD-response during the MID-task, they also found treatment-associated increases in striatal activity, including in the right NAc. These results link anhedonia and reward processing in the striatum together by showing that pramipexole treatment improves anhedonia symptoms as well as increases neuronal activity in the dopaminergic mesolimbic pathway.

A Resting-state Perspective

Above, evidence from task-based fMRI studies was discussed, where activity in the brain is observed in relation to a task that aims to activate the same cognitive processes and brain regions as a real-life situation would. The brain is also active when there is no task, i.e. when the brain is in a resting-state (Biswal, 1995). In resting-state studies, participants are asked to stay still with their eyes closed and to not think of anything in particular, but at the same time refrain from falling asleep (Raichle, 2010). Electroencephalography (EEG) studies have shown that during resting-state, a person's electrical brain activity will oscillate at a slower frequency (i.e., the number of amplitude waves or complete cycles in one second (Kane et al., 2017))- around 7.5-12.5 hz- compared to when a person is alert, during an activity or task (12.5-30 hz) (Newson & Thiagarajan, 2019). Resting-state fMRI data can be used to infer connectivity between brain regions, such as functional connectivity. Functional connectivity (FC) is inferred from a correlation of BOLD signals in spatially separated regions. It can be calculated between two specific regions of interest (ROI), or between one ROI and the rest of the brain, for a more exploratory approach (Fox & Raichle, 2007).

In depression and anhedonia, abnormal activity patterns of the NAc have not only been found during tasks but have also been detected in resting-state functional connectivity (rsFC). Ding et al. (2022) conducted a meta-and mega-analysis on the rsFC of the NAc in depression. They reported that depression was associated with decreased rsFC with the NAc and other reward processing regions, such as the medial prefrontal cortex, the ventral tegmental area, and the hippocampus. Reduced rsFC with the NAc has also been found in participants with depression and anhedonia. Wacker et al. (2009) found that anhedonia was associated with altered reward processing regions during tasks (evidence from EEG and fMRI) but also during resting-state (evidence from EEG). Anhedonia was associated with reduced resting-state activity (indicated by increased delta band activity) in the rostral anterior cingulate cortex (rACC) region (Wacker et al., 2009). Gabbay et al. (2013) compared subjects with MDD and healthy controls. They found that the MDD group had decreased rsFC between the right NAc and the middle temporal gyrus. MDD severity was negatively correlated with rsFC between the right NAc and the dorsomedial prefrontal cortex, suggesting that lower coordination between these two could predict MDD severity. Further, they also found that anhedonia severity was negatively correlated with rsFC between the left NAc and the subgenual ACC as well as the left caudate, respectively, and between the right NAc and occipital fusiform gyrus (Gabbay et al., 2013). Another study found that in participants with MDD, anhedonia severity was associated with reduced rsFC between the ventral tegmental area/substantia nigra and the NAc (Young et al., 2016).

Taken together, findings from resting-state studies suggest that compared to healthy controls, patients with MDD and anhedonia have decreased connectivity with the NAc and known reward processing areas such as the dorsomedial prefrontal cortex and anterior cingulate cortex. In theory, if reduced resting-state connectivity with the NAc underlies anhedonia symptoms, it can be suggested that said connectivity would increase if the patient was successfully treated. However, this claim cannot be made in a case-control design comparing MDD with healthy control. There is a gap in the literature for a repeated measures, pre-post comparison of NAc connectivity in patients with MDD and anhedonia.

The Current Study

Evidence from previous studies suggests that anhedonia is associated with dysfunctional reward processing—studies showing differences in reward network rsFC and activity patterns during reward-related tasks support this claim. However, these studies primarily use a case-control design, comparing brain imaging data between a group with

anhedonia and healthy controls or differences across anhedonia severity in participants with depression. To the author's knowledge, there has been no attempt to compare how functional connectivity changes as anhedonia symptoms improve in a repeated-measures design. Furthermore, it is unclear how pramipexole affects rsFC. Thus, the aim of the current study is to compare resting-state functional connectivity between the NAc and all other regions in the brain, pre- and post-pramipexole treatment in a patient sample with depression and anhedonia.

Previous studies report that rsFC in participants with depression and anhedonia is reduced compared to healthy controls (Ding et al., 2022). Thus, this study predicts that rsFC will increase in regions associated with reward processing, such as the ACC and dorsomedial prefrontal cortex, as a result of pramipexole treatment. However, due to limited previous research on the topic, the current study's hypothesis is exploratory.

Method

Participants

Participants were collected as part of a larger research project (see Ventorp et al., 2022). The current study analysed data from nine participants. Participants were recruited from outpatient clinics in Lund, Sweden. All participants were diagnosed with moderate-to-severe unipolar or bipolar depression and were on a stable dose of one or several antidepressants and/or mood stabilisers. Participants were required to score <27 on the Dimensional Anhedonia Rating scale (DARS) (inverse scale) (Rizvi et al., 2015) to take part in the study. No participant had any contraindications to MRI scanning. For a detailed description of sample characteristics, see Ventorp et al. (2022).

Procedure

For a complete description of the procedures, see Ventorp et al. (2022). Prior to treatment start, participants' baseline wellbeing was rated using the DARS, the Montgomery Åsberg Depression rating scale (MADRS) (Montgomery & Åsberg, 1979), Snaith-Hamilton Pleasure scale (SHAPS) (Snaith et al., 1995), the Apathy Evaluation scale (AES) (Marin et al., 1991), the Fatigue Severity scale (FSS) (Krupp et al., 1989), and the Insomnia Severity index (ISI) (Morin et al., 2011). Participants' wellbeing was also rated using the scales mentioned above every other week throughout the treatment period. In addition to these questionnaires, participants were screened using the Young Mania Rating scale (YMRS) (Young et al., 1978), the Questionnaire for Impulsive-compulsive Disorders in Parkinson's Disease (QUIP) (Weintraub et al., 2012), and the Problem Gambling Severity index (PGSI) (Young and Wohl,

2011) starting from week 2 of treatment and every other week until the end of the treatment period.

Pramipexole Administration

Participants continued their normal dosage of one or several antidepressants and/or mood stabilisers in combination with the pramipexole treatment. Pramipexole was administered in depot tablets once a day for 10 weeks. The dosage was titrated to a maximum of 4.5 mg salt/day. In week 1, all participants took 0.375 mg salt/day and 0.75 mg salt/day in week 2, followed by an increase of 0.75 mg salt/day each week until week 7 when participants continued with a stable dose of 4.5 mg salt/day until the end of the study. Dosage increase was stopped in the event of reported side effects and continued the following week unless side effects remained. Dosage increase was also stopped if a participant scored ≥50% on the MADRS or >40 on the DARS and the participant was asked to continue with that dosage until the end of the study.

Imaging Data Acquisition and Pre-processing

Imaging Acquisition

Subjects were asked to participate in two scanning sessions, one prior to treatment start and one after 10 weeks of treatment. Each session took approximately 45 minutes and consisted of a survey-scan, two B0-field maps (one for shimming parameters and one for unwarping), a T1-weighted scan, one task-based functional scan (MID), and one resting-state functional scan. The current study only used the T1-weighted anatomical image, and the resting-state scans for analysis.

During the resting-state scan, participants were asked to rest with their eyes closed without falling asleep or thinking about anything in particular. The resting-state scan took 10 minutes (400 volumes, TR=1500 ms). Participants were placed in a supine position with their heads in a 32-channel head-coil. No particular implementations were used to reduce movement, but subjects were instructed to remain as still as possible throughout the scan. Due to the loud noise from the scanner, participants wore protective earplugs. Participants were also given a hand-held alarm button to indicate if they wanted to discontinue the examination.

Scanning took place at the Lund University Bioimaging Centre using a 7T whole body MR scanner (Philips Achieva, Philips Medical Systems, Best, The Netherlands). The anatomical images were acquired with the following parameters; repetition time (TR) of 5.0 ms; echo time (TE) = 1.97 ms; flip angle = 6°; voxel size = 1.0×1.0×1.0 mm^3. The BOLD

functional data was acquired using a simultaneous multi-slice echo-planar imaging (SMS-EPI) sequence (TR=1500 ms; TE=25 ms; flip angle= 55°; voxel size=2.0×2.0×2.0 mm^3; slice gap =0.2 mm; slices=50; multi-slice acceleration factor=2; SENSE acceleration factor=3).

Pre-processing

MRI-images need to undergo a series of pre-processing and denoising steps before being analysed. For the current thesis the following pre-processing steps were implemented. The first five volumes were removed. This is common practice as it takes a few seconds for the hydrogen molecules to align with the magnetic field. The structural and functional data were pre-processed using the default pipeline in the CONN toolbox for Matlab (Nieto-Castanon, 2020; Whitfield-Gabrieli & Nieto-Castanon, 2012) (www.nitrc.org/projects/conn). This pre-processing pipeline included 6 steps. (1) The functional data were realigned and unwarped with subject motion estimation and correction. This was done using the SPM realign and unwarp procedure. Realignment (or correction by co-registration) rotate the images to align them- with the first scan of the first session as a reference image. This step is done in case the participant has moved during scanning (Nieto-Castanon, 2020). (2) Slice-dependent delays were corrected by using slice-timing correction. fMRI scans are acquired using echo planar imaging (EPI) (i.e., data is collected as two-dimensional slices). Slices cannot be collected simultaneously; therefore, there will be a temporal misalignment of slices within one volume (Parker & Razlighi, 2019). In the current study, slices were collected using a simultaneous multi-band EPI sequence. Slice-timing correction is done to align the slices to a common temporal reference point (Parker & Razlighi, 2019). (3) Outlier data-points in the functional data were identified using ART-based (Artifact Detection Tools) identification. Data-points were considered outliers if movement parameters showed a framewise displacement above 0.9 mm or were above 5 standard deviations in global BOLD signal change. Outlier data points were later removed from the time-series during the denoising step, i.e. before functional connectivity analysis. (4) The functional and structural images were segmented into grey matter, white matter, and cerebrospinal fluid (CSF). (5) The functional and structural data were normalised to the Montreal Neurological Institute (MNI) space. Following the segmentation and normalisation, the data were resampled to 2 mm isotropic voxels with the default IXI-549 tissue probability map template in SPM. (6) The functional data was smoothed with a full-width half maximum (FWHM) Gaussian Kernel; this will increase the BOLD signal-to-noise ratio (Nieto-Castanon, 2020).

Denoising

In addition to the pre-processing steps, the functional data was denoised. Denoising is particularly relevant for resting-state data as it tends to be more susceptible to noise (Birn, 2012; Weiler et al., 2022). Denoising was done in two steps, first linear regression followed by temporal band-pass filtering. The functional data was denoised using the standard denoising pipeline in the CONN toolbox. Linear regression (ordinary least squares) was used to identify and remove confounding factors from the BOLD data. An aCompCor procedure (Behzadi et al., 2007) was then implemented (Nieto-Castanon, 2020). The confounding noise components were white matter time-series (5 components), CSF time-series (5 components), the 6 motion parameters estimated during the realignment step as well as their first derivative (12 factors), outlier scans identified during artefact detection (individual for each subject, all below 20 factors), effects of session (4 factors), and linear trends within each functional run (2 factors). A high-pass frequency filter was also applied as a regressor to the BOLD time-series (0.008 inf). A total of 46 volumes were scrubbed across participants and sessions, range 0-20 (M=2.56, SD=5.33).

Analysis

First-level Analysis

All analyses were conducted using the CONN toolbox for Matlab. In first-level analysis, bivariate correlation maps for all subjects in each session are obtained to calculate functional connectivity. A general linear model (GLM) was conducted, including movement parameters (realignment, quality control time-series, and scrubbing), white matter, and cerebrospinal fluid as covariates to be regressed out. Functional connectivity was calculated between pre-defined seeds and all other voxels in the brain. Two seed regions of interest (ROI) were used: the left and right accumbens, entered bilaterally. The ROI seeds were defined using the Harvard-Oxford cortical and subcortical atlas (see Desikan et al., 2006; Frazier et al., 2005; Goldstein et al., 2007; Makris et al., 2006). Individual seed-based connectivity maps for each subject and each session were obtained by averaging the time-series of the voxels within each seed region (left and right accumbens). The mean time-series were then correlated with the time-series of all other voxels using Pearson's correlation coefficient. The seed-based bivariate correlation maps were normalised by converting them into z-maps using Fisher's r-to-z transformation (Lowe et al., 1998; Nieto-Castanon, 2020).

Group-level Analysis

In group-level analysis, the functional connectivity established in the first-level analysis for each participant and session is averaged across participants within each session. A GLM was conducted for each voxel, with first-level connectivity as the dependent variable and session (pre and post) as independent variables. A F-test determined the strength of connectivity.

Between-sessions Comparison

The pre-post comparison was part of the group-level GLM. The interaction between the ROI time-series and the group variable (session) was tested, and strength is determined with an F-test. This is done by conducting separate multiple regression models for each ROI (left and right accumbens) time-series (outcome variable). The predictor variables were (1) the seed ROI BOLD time-series, (2) the group effect (i.e., the group boxcar time-series), a canonical hemodynamic response function was used to model the hemodynamic response function, (3) the interaction term between (1) and (2).

The between-conditions contrast was (-1 1) and connectivity direction was calculated as an effect size representing the average difference in the Fisher-transformed correlation coefficients (functional connectivity) between the pre-post conditions, for each pair of ROIs. This analysis attempts to estimate the change in rsFC between the two sessions (i.e. before and after treatment), and the direction of the change.

Correction for Multiple Comparisons

Setting significance thresholds or false positive rates for p-values (alpha-level) is a common practice to minimise the risk of reporting false positives. However, in mass univariate analysis of fMRI data, analyses are made at each voxel. As there can be more than 100,000 voxels in one dataset, even a restrictive alpha-level of 0.001 would make the results vulnerable to false positive results (Lieberman & Cunningham, 2009). Therefore, the threshold needs to be corrected for multiple comparisons. This is also done in non-fMRI data analyses, usually using Bonferroni correction (i.e., the alpha-level divided by the number of tests conducted). However, Bonferroni correction is not suitable for fMRI data analysis as it assumes that all analyses are independent but, voxel time courses are not entirely independent of one another, as nearby voxels are usually highly correlated (Woo et al., 2014).

Cluster-level correction is a common way that fMRI data analyses are controlled for multiple comparisons (Woo et al., 2014). The logic is that false positives are random and, therefore, less likely to occur in a cluster (Lieberman & Cunningham, 2009; Woo et al., 2014).

This is done in two steps, first by setting a voxel-level threshold and then applying a cluster-level threshold. The voxel-level threshold determines the significance level (i.e. *p*-value) a voxel must reach for that voxel to be considered as part of a cluster. The cluster-level threshold sets the significance-level for how large a cluster must be to be considered significant (Woo et al., 2014).

Several methods have been developed for correction for multiple comparisons of fMRI data (Han et al., 2019). Family-wise error (FWE) correction and false discovery rate (FDR) correction are two common methods. FWE-correction is a more restrictive option that attempts to remove all the type I errors (Lieberman & Cunningham, 2009). In FWE-correction, the threshold value is the percentage of risk that there are false positives (Bennett et al., 2009). FDR-correction is less restrictive; it attempts to limit the type I errors. The aim is to minimise false reports without compromising true results. Because FDR-correction is less restrictive, it has been argued that this method should be preferred over FWE-corrections as by focusing on only one type of error, one is likely to risk increasing the amount of the other error (Han et al., 2019; Lieberman & Cunningham, 2009).

Ultimately, the choice of method for correction of multiple comparisons for *p*-value thresholds depends on the study. The current study used a cluster-corrected approach and with a voxel-level threshold of $p<.001$ (uncorrected) and a cluster-level threshold of $p<.05$ (FDR corrected) for all analyses conducted. These thresholds were chosen as the small sample size put the study at risk for type II error (false negatives) if the thresholds are too restrictive.

Ethical Statement

The study design followed the principles laid out by the World Medical Association (WMA) declaration of Helsinki (World Medical Association, 2013) and the International Council for Harmonisation (ICH) Good Clinical Practice (GCP) guidelines. The Swedish Ethical Review Authorities (#2019-02843) and the Swedish Medical Products Agency (EduraCT 2019-001907-19) approved the study prior to data collection.

The study procedures were planned by medical experts and supervised by qualified monitors from Clinical Studies Sweden. Pramipexole is approved by the European Medicines Agency (EMA). The administration was open-labelled, and all participants were fully informed of any potential side-effects. Although pramipexole is primarily prescribed as a treatment of Parkinson's disease, there have been numerous successful trials that have administered pramipexole to MDD patients without Parkinson's disease (Tundo et al., 2019; Tundo et al., 2022).

MRI is a non-invasive method. The imaging data collection was conducted by experienced personnel and followed all safety precautions. All participants were fully informed and gave written consent prior to taking part in the study.

Results

Pramipexole was well tolerated with some reported side effects. Participants' scores on the DARS, MADRS, and SHAPS had significantly improved after 10 weeks of treatment (all $p<.01$), indicating a treatment effect of pramipexole. For further details, see Ventorp et al. (2022).

ROI-to-voxel Analysis

Main Effects Pre-treatment

In the pre-treatment session there was significant functional connectivity between the bilateral NAc seeds and 20 clusters; both positive (N=15) and negative (N=4) correlations were found. In one instance, the direction of the correlation was different depending on the ROI, where there was negative correlation with the right accumbens seed, and a positive correlation with the left accumbens seed. This cluster covered the bilateral precuneus (F=11.55, cluster size=85 voxels, peak voxel at xyz-coordinates 2, -74, 46). The strongest positive connectivity (indicated by effect size >.2) was found in a cluster covering and surrounding the bilateral subcallosal cortex, bilateral putamen, bilateral caudate, bilateral NAc, bilateral insular cortex, bilateral orbitofrontal cortex, bilateral pallidum, bilateral frontal pole and left thalamus (F=116.50, cluster size=3532 voxels, peak voxel at xyz-coordinates 8, 10, -02). See figure 1 for the significant clusters of rsFC main effects. For a list of all significant clusters, see table A1 in appendix A.

Main Effects Post-treatment

In the post-treatment session, there was significant functional connectivity between the bilateral NAc seeds and 17 clusters; both positive (N=7) and negative (N=8) correlations were found. In two clusters, the direction of the correlation was different depending on the ROI. In one cluster covering the right frontal pole, the right accumbens seed was negatively correlated, whilst the left accumbens seed was positively correlated (F=18.23, cluster size=137 voxels, peak voxel at xyz-coordinates 34, 44, 40). In the other cluster, the opposite was found where the right accumbens seed was positively correlated, but the left accumbens seed was negatively correlated, this cluster covered the left frontal pole (F=16.21, cluster size=67 voxels,

peak voxel at xyz-coordinates -12, 46, 42). The strongest positive connectivity (indicated by effect size >.15) was found in a cluster covering and surrounding the bilateral NAc, bilateral caudate, bilateral putamen, bilateral anterior cingulate gyrus, bilateral paracingulate gyrus, bilateral subcallosal cortex, bilateral medial frontal cortex, bilateral frontal pole, bilateral orbitofrontal cortex, bilateral thalamus, bilateral insular cortex, bilateral pallidum, bilateral amygdala (F=47.09, cluster size=8486 voxels, peak voxel at xyz-coordinates 8, 12, -04). See figure 1 for the significant clusters of rsFC main effects. For a list of all significant clusters, see table A2 in appendix A.

Figure 1

Strength of Connectivity in Clusters of rsFC with the NAc, Pre-and Post-treatment

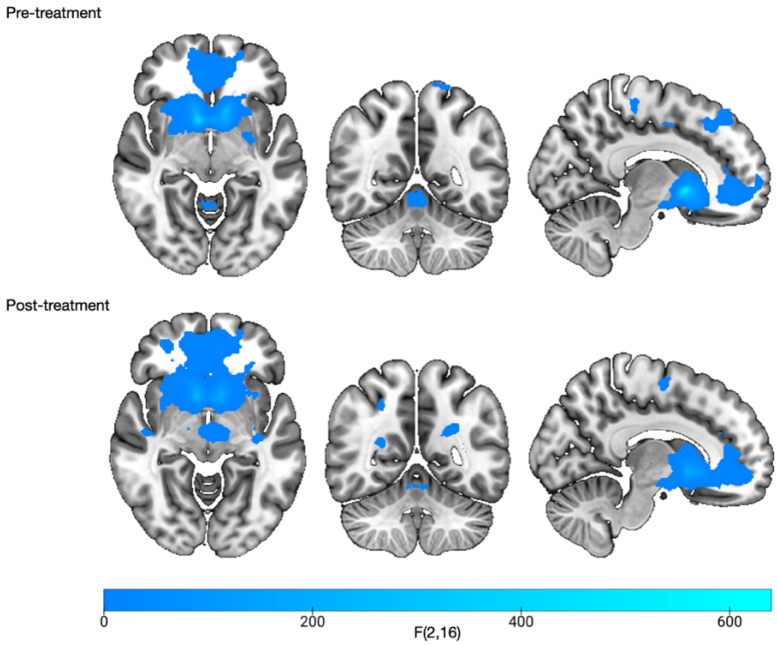

Note. rsFC of the NAc pre-and post-treatment. Only clusters passing the threshold for multiple comparisons are shown. Clusters are displayed on an MNI-template and colour-coded to indicate strength of the effect (F-statistic). Images were created using MRIcroGL (https://www.nitrc.org/projects/mricrogl).

Session Comparison

When comparing the functional connectivity pre- and post-treatment, two significant clusters were found, see figure 2. There was a significant difference in functional connectivity between the bilateral NAc and the right lingual gyrus (F=14.87, cluster size=95 voxels, peak voxel at xyz-coordinates 20, -48, -02). Prior to treatment, the functional connectivity was

positive; however, post-treatment the direction of the connectivity was negative, see figure 3. The second cluster covered some of the left intracalcarine cortex. Connectivity with this cluster was also positive pre-treatment, but negative post-treatment (F=24.21, cluster size=89 voxels, peak voxel at xyz-coordinates -28, -68, 0). See table 1 for *p*-values. Note that the left intracalcarine cortex only accounted for 17% of the cluster. 9% of the cluster was covering the precuneous, and the remaining 74% of this cluster mostly covered white matter and could therefore not be classified by the Harvard-Oxford cortical and subcortical atlas (Desikan et al., 2006; Frazier et al., 2005; Goldstein et al., 2007; Makris et al., 2006).

Figure 2

Strength of Group Differences in rsFC with the NAc Pre-and Post-pramipexole Treatment

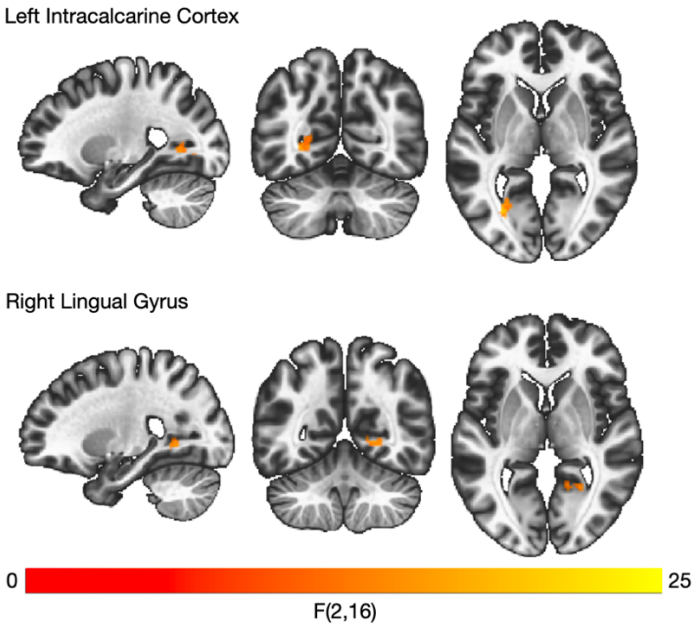

Note. Repeated-measures group comparison between the pre- and post-treatment rsfMRI scans. Compared to the pre-treatment scans, the post-treatment scans showed a significant difference in rsFC of the NAc with the right lingual gyrus and left intracalcarine cortex. Clusters are displayed on an MNI-template and are colour-coded to indicate the strength of the effect (F-statistic). Only clusters passing the threshold for multiple comparisons are shown. Images are generated using the CONN toolbox.

Figure 3

Effect Sizes of Group Differences in rsFC with the NAc Pre-and Post-treatment

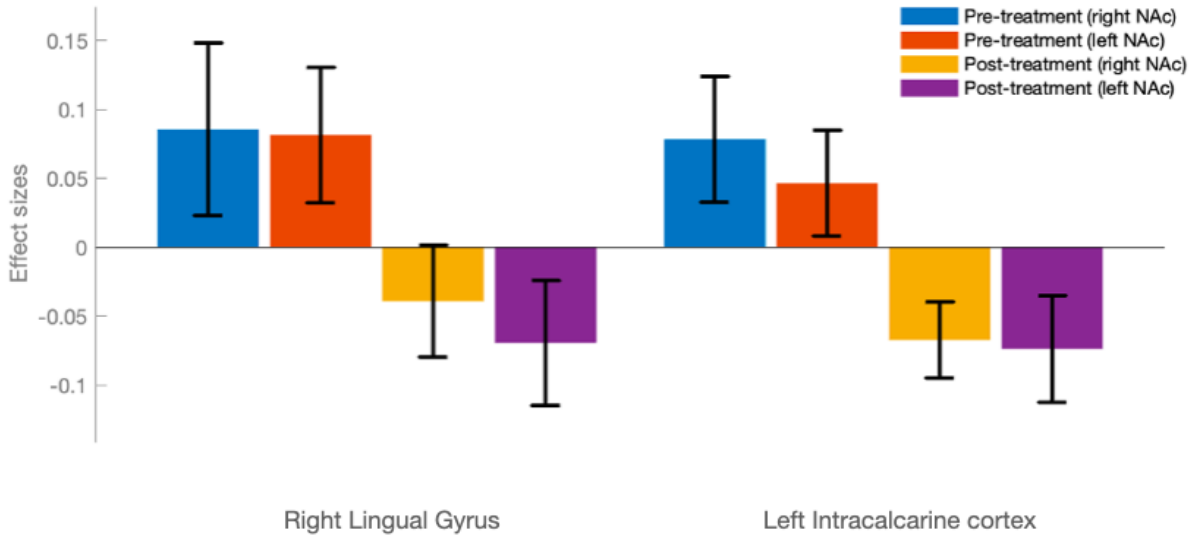

Note. Bars showing effect sizes (i.e., mean difference in Fisher-transformed z-scores) with 90% confidence intervals. Repeated-measures groups comparison between the pre-and post-treatment rsfMRI scans. Compared to the pre-treatment scans, the post-treatment scans showed a significant difference in rsFC of the NAc with the right lingual gyrus and left intracalcarine cortex. The graph was generated using the CONN toolbox.

Table 1

The Significant Between-session Differences in Resting-state Functional Connectivity with the NAc

Cluster location	Hemisphere	Peak voxel (MNI) coordinates			Number of voxels	F-value	*P*-value (uncorrected)	*P*-value (FDR)
		X	Y	Z				
Lingual gyrus	Right	+20	-48	-2	95	14.87	<0.001	0.001
Intracalcarine cortex	Left	-28	-68	0	89	24.21	0.003	0.003

Note. Clusters of rsFC of the NAc ROI (bilateral) with a significant difference in rsFC pre-and post-treatment.

Discussion

The aim of this study was to explore how rsFC of the NAc would change as a result of 10 weeks of pramipexole treatment in a sample of patients with depression and anhedonia. Given the novelty of the current design and lack of extensive evidence pointing one way, this study should be considered as largely exploratory. However, previous studies have generally found reduced rsFC between the ventral striatum and various brain regions involved in reward

processing and salience detection in patients with depression and anhedonia as compared to healthy controls (Ding et al., 2022; Gabbay et al., 2013; Young et al., 2016). This supports an tentative hypothesis that successful pharmacological treatment would normalise this discrepancy, and thus result in increased rsFC between NAc and other regions. Previously published results on this sample found that scores on anhedonia and depression scales had improved after ten weeks of treatment as well as increased activity in the striatum during the MID task, indicating a treatment effect of pramipexole (Ventorp et al., 2022). This thesis builds on these results but focuses instead on changes in rsFC before and after treatment. The main effects analyses revealed significant functional connectivity with the NAc and expected regions, such as the ACC, medial prefrontal cortex and orbitofrontal cortex (Ding et al., 2022), see appendix A for full list. This supports the validity of the brain imaging data in that it demonstrates the expected pattern of connectivity between the ROIs used and other brain regions. After comparing pre-and post-treatment scans, decreases in rsFC was observed in two clusters in the posterior part of the cortex. In both these clusters, rsFC were initially positively correlated with the NAc but became negatively correlated post-treatment. These clusters were located in the right lingual gyrus and a cluster in the left hemisphere covering the intercalcarine gyrus. Thus, there are two key findings of the current study. First, the rsFC of the NAc changed from positive to negative in the lingual gyrus and intracalcarine cortex. Second, there were no significant differences in the rsFC of the NAc and known reward processing regions in the brain.

Pre- and Post-treatment Differences in rsFC

The rsFC analysis showed that both clusters that were significantly different in rsFC between the pre-and post-treatment sessions had gone from a positive rsFC (indicated by a positive correlation coefficient) to a negative correlation (also referred to as an anticorrelation). Functional connectivity is the statistical dependency between time-series in voxels. Two brain regions with a positive rsFC are interpreted to have similar activation patterns and to be synchronised. Negative correlations can be interpreted as deactivation of the regions during resting-state. For example, the default mode network is a resting-state network with regions that activate together during resting-state and deactivate together during tasks (Fox et al., 2005; Martinez-Gutierrez et el., 2022).

There have been discussions in the literature regarding if and to what extent negative correlations in resting state data should be interpreted as meaningful results. Shehzad et al. (2009) assessed the test-retest reliability of functional connectivity analyses. They found greater

reliability of positive correlations compared to negative correlations. Furthermore, there have been suggestions that negative correlations occur due to global signal correction during pre-processing and denoising, and are therefore not meaningful (Fox et al., 2009; Murphy et al., 2009; Saad et al., 2012). However, there have also been several counterarguments asserting that negative correlations cannot be spurious as research suggests that they serve a physiological and neuronal purpose (Demertzi et al., 2022). Additionally, Chai et al. (2012) compared results from data where global signal regression had been used to remove noise and results from data that had used an alternative method. They found similar negative correlations in both analyses, indicating that negative correlations are valid results.

Demertzi et al. (2022) proposed that negative correlations should be interpreted as neural inhibition, where anticorrelated networks (i.e., regions that deactivate together) are indirect products of neural inhibition which overall affect metastability and balanced cortical activity. They argue that inhibition between brain regions will lead to a disruption in the balance of excitation and inhibition in the brain, indirectly resulting in negative correlations (Demertzi et al., 2022). According to this view, the emergence of negative correlations observed in the current study could be interpreted as increased inhibitory activity between the NAc and the right lingual gyrus and left intra calcarine cortex, respectively, and that pramipexole treatment aided in the emergence of negative correlations between the regions.

The Right Lingual Gyrus

This study found that rsFC between the NAc and right lingual gyrus was significantly different in the post-treatment scan compared to the pre-treatment scan. The lingual gyrus is located in the medial occipital lobe, it has been associated with functions including visual processing, linguistic processing, visual memory, and emotional processing (Palejwala et al., 2021). Several studies have found abnormal resting-state functional connectivity with the lingual gyrus in patients with MDD. Veer et al. (2010) conducted a whole-brain resting-state functional connectivity analysis in patients with MDD and healthy controls. They found reduced rsFC with the bilateral lingual gyrus within a network in the medial occipital cortex, including ventromedial occipital temporal areas, in the MDD group compared to healthy controls. Another study found increased rsFC between the lingual gyrus and anterior hippocampus in patients with MDD and bipolar disorder compared to healthy controls (Fateh et al., 2019). In a sample of patients with Alzheimer's disease (AD), Liu et al. (2017) found reduced rsFC between the dorsal ACC and lingual gyrus in AD patients with MDD compared to AD patients without MDD. Luo et al. (2022) reported that participants with MDD and

childhood trauma had reduced rsFC between the left lingual gyrus and the right calcarine cortex. There have also been studies relating antidepressant treatments with lingual gyrus, Jung et al. (2014) found that the grey matter volume of the lingual gyrus could predict antidepressant treatment effect. Participants who responded to their treatment had greater grey matter volume in the lingual gyrus than participants who did not respond to the antidepressant therapies. Taken together, this evidence suggests that abnormal rsFC of the lingual gyrus is relevant to model the neurobiology of depression.

Although the change in rsFC between the NAc and lingual gyrus was not expected initially, it is not completely surprising. A recent study by Hu et al. (2023) compared rsFC with the core and shell of the NAc between patients with depression and anhedonia and healthy controls. They reported that the patient sample showed reduced rsFC between the left NAc core and right lingual gyrus compared to healthy controls. In the MDD sample, scores on an anticipatory anhedonia measurement (anhedonia severity indicated by a lower score) were positively correlated with the rsFC between the left NAc core and the right lingual gyrus, indicating that the reduced positive correlation between the NAc and lingual gyrus was associated with greater anhedonia severity (Hu et al., 2023). Interestingly, the data published by the authors also suggest that among participants on the lower end of the anticipatory anhedonia scale (indicating more severe anhedonia), the rsFC between the left NAc and right lingual gyrus was negative. In participants with higher scores on the anticipatory anhedonia scale (indicating less severe anhedonia), on the other hand, the correlation was positive. This change in the directionality of the rsFC was not considered by the authors or tested; however, the results are the opposite of the current study's findings, where a decrease in anhedonic symptoms after treatment were accompanied with a change from positive to negative functional connectivity between NAc and lingual gyrus. Further replication and analysis of these findings are needed to explore if the decreased resting-state relationship between the NAc and lingual gyrus after treatment is meaningful, or spurious.

The Left Intracalcarine Cortex

There was also a significant difference in rsFC of the NAc with the left intracalcarine cortex. Like the lingual gyrus, the direction of connectivity of this cluster shifted from positive prior to treatment, to negative post-treatment. Above, this cluster is labelled as the left intracalcarine cortex however, it should be noted that this cluster only encompassed 17% of the left intracalcarine cortex. In turn, the cluster only accounted for 2% of the entire intracalcarine cortex, thus making the interpretation of this result limited as discussion of the intracalcarine

cortex would be misleading. The remaining 74% of this cluster mostly covered white matter and was therefore not classified by the Harvard-Oxford cortical and subcortical atlas (Desikan et al., 2006; Frazier et al., 2005; Goldstein et al., 2007; Makris et al., 2006).

Given the placement of this cluster, it can be suggested that it is a type II error, i.e., a false positive result. Random, spurious results are not uncommon in fMRI data, given the great number of analyses that are often conducted on small sample sizes (Bennet et al., 2009; Cremers et al., 2017). Spurious correlations can also be a result of movement during scanning that is not accounted for in preprocessing and denoising (Power et al., 2012). Furthermore, the limitations of the present study puts the current results at higher risk of both type I and II error, these limitations are further discussed below.

An additional indication that the difference in connectivity may not be meaningful is that there were no significant main effects between the NAc and the right lingual gyrus or left intracalcarine cortex. In the current study, the significant differences in rsFC between the pre- and post-treatment scanning sessions are attributed to the switch in direction of correlation between the bilateral NAc and the right lingual gyrus, and left intracalcarine cortex respectively. However, rsFC between the NAc and the right lingual gyrus and left intracalcarine cortex were not found in the pre-and post-treatment main effects. The lack of significant main effects in these regions could suggest that the detected pre-post differences are not true effects. For example, it is possible that the rsFC in one or both of the sessions was a random, spurious result that was then found to be significantly different from the other. On the other hand, the rsFC main effects could have been too subtle to be detected in the current analysis. In a similar manner, the current study did not find a significant difference in rsFC between the NAc and reward regions, as was predicted.

Connectivity Between The NAc and Other Reward Regions

The current results are inconsistent with the prediction made based on previous observations. Research comparing participants with MDD and anhedonia and healthy controls have found significantly reduced rsFC of the NAc and reward processing regions, such as the sgACC and caudate, in the MDD sample (e.g., Gabbay et al., 2013). It was predicted that improvement in anhedonia and MDD symptoms would elicit a change in rsFC between the NAc and these regions. The current study did not find evidence that would indicate this. This could be attributed to the limitations of the study, such as the low statistical power, see discussion below. It can also be attributed to the *p*-value thresholds that were set and the methods for correction for multiple comparisons used. It has been suggested that uncorrected

p-value thresholds are not appropriate (Bennett et al., 2009), while others have argued that as restrictive correction methods put the study at risk of missing meaningful results, and more effort should be put on larger sample sizes and replication studies to minimise type I error, without risking type II error (Lieberman & Cunningham, 2009). The current study used a cluster-corrected approach and with a voxel-level threshold of $p<.001$ (uncorrected) and a cluster-level threshold of $p<.05$ (FDR corrected) for all analyses conducted. Although these are relatively generous thresholds, they could remove small effects from the results.

Moreover, the current study did not distinguish between the NAc core (dorsolateral NAc) and shell (ventromedial NAc) in the analysis. However, some researchers in the field have advocated that they should be separate ROIs in connectivity analyses (Gorwood, 2008; Xia et al., 2017). It has been suggested that the NAc core and shell have different functions in reward processing (Ambroggi et al., 2011; Castro & Berridge, 2014) and dopamine firing (Gorwood, 2008). Differences between the NAc core and shell have also been found in rsFC analyses. For example, Liu et al. (2021) found that rsFC of the core and shell, respectively, was different when comparing participants with MDD and healthy controls. In addition to differences in rsFC strength between the NAc core and shell, Liu et al. found decreased rsFC between the right NAc core and left mid-anterior orbitofrontal cortex, and the right inferior parietal lobe in the MDD group, compared to healthy controls. They also reported decreased rsFC between the left NAc core and right middle frontal gyrus in the MDD group, compared to healthy controls. However, they found no group effects in rsFC of the NAc shell seed. Hu et al. (2023), as mentioned above, also found differences between rsFC of the NAc core and shell subregions in MDD. In addition to decreased connectivity between the left NAc core and lingual gyrus, the authors reported decreased connectivity between the right NAc core and right inferior frontal gyrus/insula in the MDD group, compared to healthy control. They also found decreased rsFC between the right NAc shell and right middle frontal gyrus/superior frontal gyrus in the MDD group, compared to healthy controls. Hu et al. also found evidence suggesting that consummatory anhedonia was associated with rsFC of the NAc shell, whilst anticipatory anhedonia was associated with rsFC of the NAc core. Both Liu et al. (2021) and Hu et al. (2023) findings suggest that there are distinct rsFC patterns of the NAc shell and core. In the current study, the time-series of all voxels within the NAc boundaries were averaged and correlated with all other voxels. This may have diminished connectivity that would have been found if the NAc ROI had been divided into core and shell.

Limitations and Future Directions

The current study is not without limitations. First, the small sample size and low statistical power (i.e., the probability of rejecting the null when it is false) put this study at risk of type I and II error. In studies with small sample sizes, random connectivity is more likely to affect the overall results (Lieberman & Cunningham, 2009). fMRI studies tend to have a large number of variables and analyses but with a small sample size, making low statistical power prevalent in the literature (Cremers et al., 2017). Low statistical power compromises the likelihood that a statistically significant finding reflects a true effect. In an otherwise ideal study, low statistical power will still risk type II error, low positive predictive value (i.e., the probability that a significant finding is a true effect), and exaggerated effect sizes on significant results that are true effects (Button et al., 2013). Furthermore, with low statistical power, smaller effects and weaker connectivity are less likely to be detected. Thus, the current study should be replicated with a larger sample size.

Second, the current study does not allow for causal inference: the administration was open-labelled and there were no control or placebo groups. Thus, it would be premature to conclude that differences pre-to post-treatment are attributed to the specific pharmacological effects of pramipexole. In order to determine if changes indeed are specific to the treatment, placebo-controlled studies need to be performed.

The limitations aside, the current results are consistent with previous observations that connectivity between the lingual gyrus and NAc may play a role in the underlying pathophysiology of depression and anhedonia. However, the role of the lingual gyrus is often not considered in large-scale reviews and meta-analyses on the topic. Furthermore, research that has reported significant differences in connectivity of the lingual gyrus as it relates to depression and anhedonia have used other seed ROIs. Future research should consider conducting a seed-to-voxel analysis with the lingual gyrus as ROI.

Conclusion

In conclusion, this was the first attempt at comparing how rsFC of the NAc changed as a result of pramipexole treatment within a sample of patients with depression and anhedonia. The study found that rsFC between the NAc and the lingual gyrus, and the intracalcarine cortex shifted from a positive correlation prior to treatment, to a negative correlation post treatment. These results are somewhat inconsistent with previous findings however, this may be attributed to the study's limitations. A replication of the current design, adding a control group and a larger sample, is needed. Nevertheless, the current results add to the growing literature suggesting that

the lingual gyrus may play a fundamental role in the mechanisms of anhedonia and depression. However, further research is needed to establish this.

References

Admon, R., Kaiser, R. H., Dillon, D. G., Beltzer, M., Goer, F., Olson, D. P., Vitaliano, G., & Pizzagalli, D. A. (2017). Dopaminergic Enhancement of Striatal Response to Reward in Major Depression. *American Journal of Psychiatry*, *174*(4), 378–386. https://doi.org/10.1176/appi.ajp.2016.16010111

Ambroggi, F., Ghazizadeh, A., Nicola, S. M., & Fields, H. L. (2011). Roles of Nucleus Accumbens Core and Shell in Incentive-Cue Responding and Behavioral Inhibition. *The Journal of Neuroscience*, *31*(18), 6820–6830. https://doi.org/10.1523/JNEUROSCI.6491-10.2011

American Psychiatric Association. (2013). *Diagnostic and Statistical Manual of Mental Disorders*. American Psychiatric Association. https://doi.org/10.1176/appi.books.9780890425596

Antonini, A., Barone, P., Ceravolo, R., Fabbrini, G., Tinazzi, M., & Abbruzzese, G. (2010). Role of Pramipexole in the Management of Parkinson's Disease. *CNS Drugs*, *24*(10), 829–841. https://doi.org/10.2165/11585090-000000000-00000

Auerbach, R. P., Millner, A. J., Stewart, J. G., & Esposito, E. C. (2015). Identifying differences between depressed adolescent suicide ideators and attempters. *Journal of Affective Disorders*, *186*, 127–133. https://doi.org/10.1016/j.jad.2015.06.031

Auerbach, R. P., Pisoni, A., Bondy, E., Kumar, P., Stewart, J. G., Yendiki, A., & Pizzagalli, D. A. (2017). Neuroanatomical Prediction of Anhedonia in Adolescents. *Neuropsychopharmacology*, *42*(10), 2087–2095. https://doi.org/10.1038/npp.2017.28

Behzadi, Y., Restom, K., Liau, J., & Liu, T. T. (2007). A component based noise correction method (CompCor) for BOLD and perfusion based fMRI. *NeuroImage*, *37*(1), 90–101. https://doi.org/10.1016/j.neuroimage.2007.04.042

Bennett, C. M., Wolford, G. L., & Miller, M. B. (2009). The principled control of false positives in neuroimaging. *Social Cognitive and Affective Neuroscience*, *4*(4), 417–422. https://doi.org/10.1093/scan/nsp053

Birn, R. M. (2012). The role of physiological noise in resting-state functional connectivity. *NeuroImage*, *62*(2), 864–870. https://doi.org/10.1016/j.neuroimage.2012.01.016

Biswal, B., Zerrin Yetkin, F., Haughton, V. M., & Hyde, J. S. (1995). Functional connectivity in the motor cortex of resting human brain using echo-planar mri. *Magnetic Resonance in Medicine*, *34*(4), 537–541. https://doi.org/10.1002/mrm.1910340409

Borsini, A., Wallis, A. S. J., Zunszain, P., Pariante, C. M., & Kempton, M. J. (2020). Characterizing anhedonia: A systematic review of neuroimaging across the subtypes of reward processing deficits in depression. *Cognitive, Affective, & Behavioral Neuroscience*, *20*(4), 816–841. https://doi.org/10.3758/s13415-020-00804-6

Button, K. S., Ioannidis, J. P. A., Mokrysz, C., Nosek, B. A., Flint, J., Robinson, E. S. J., & Munafò, M. R. (2013). Power failure: why small sample size undermines the reliability of neuroscience. *Nature Reviews Neuroscience*, *14*(5), 365–376. https://doi.org/10.1038/nrn3475

Castro, D. C., & Berridge, K. C. (2014). Advances in the neurobiological bases for food 'liking' versus 'wanting.' *Physiology & Behavior*, *136*, 22–30. https://doi.org/10.1016/j.physbeh.2014.05.022

Chai, X. J., Castañón, A. N., Öngür, D., & Whitfield-Gabrieli, S. (2012). Anticorrelations in resting state networks without global signal regression. *NeuroImage*, *59*(2), 1420–1428. https://doi.org/10.1016/j.neuroimage.2011.08.048

Chernoloz, O., Mansari, M. El, & Blier, P. (2009). Sustained Administration of Pramipexole Modifies the Spontaneous Firing of Dopamine, Norepinephrine, and Serotonin Neurons in the Rat Brain. *Neuropsychopharmacology*, *34*(3), 651–661. https://doi.org/10.1038/npp.2008.114

Cremers, H. R., Wager, T. D., & Yarkoni, T. (2017). The relation between statistical power and inference in fMRI. *PLOS ONE*, *12*(11), e0184923. https://doi.org/10.1371/journal.pone.0184923

Demertzi, A., Kucyi, A., Ponce-Alvarez, A., Keliris, G. A., Whitfield-Gabrieli, S., & Deco, G. (2022). Functional network antagonism and consciousness. *Network Neuroscience*, *6*(4), 998–1009. https://doi.org/10.1162/netn_a_00244

Der-Avakian, A., & Markou, A. (2012). The neurobiology of anhedonia and other reward-related deficits. *Trends in Neurosciences*, *35*(1), 68–77. https://doi.org/10.1016/j.tins.2011.11.005

Desikan, R. S., Ségonne, F., Fischl, B., Quinn, B. T., Dickerson, B. C., Blacker, D., Buckner, R. L., Dale, A. M., Maguire, R. P., Hyman, B. T., Albert, M. S., & Killiany, R. J. (2006). An automated labeling system for subdividing the human cerebral cortex on MRI scans into gyral based regions of interest. *NeuroImage*, *31*(3), 968–980. https://doi.org/10.1016/j.neuroimage.2006.01.021

Ding, Y.-D., Chen, X., Chen, Z.-B., Li, L., Li, X.-Y., Castellanos, F. X., Bai, T.-J., Bo, Q.-J., Cao, J., Chang, Z.-K., Chen, G.-M., Chen, N.-X., Chen, W., Cheng, C., Cheng, Y.-Q., Cui, X.-L., Duan, J., Fang, Y.-R., Gong, Q.-Y., … Guo, W.-B. (2022). Reduced nucleus accumbens functional connectivity in reward network and default mode network in patients with recurrent major depressive disorder. *Translational Psychiatry*, *12*(1), 236. https://doi.org/10.1038/s41398-022-01995-x

Dunlop, B. W., & Nemeroff, C. B. (2007). The Role of Dopamine in the Pathophysiology of Depression. *Archives of General Psychiatry*, *64*(3), 327. https://doi.org/10.1001/archpsyc.64.3.327

Fateh, A. A., Long, Z., Duan, X., Cui, Q., Pang, Y., Farooq, M. U., Nan, X., Chen, Y., Sheng, W., Tang, Q., & Chen, H. (2019). Hippocampal functional connectivity-based discrimination between bipolar and major depressive disorders. *Psychiatry Research: Neuroimaging*, *284*, 53–60. https://doi.org/10.1016/j.pscychresns.2019.01.004

Fawcett, J., Rush, A. J., Vukelich, J., Diaz, S. H., Dunklee, L., Romo, P., Yarns, B. C., & Escalona, R. (2016). Clinical Experience With High-Dosage Pramipexole in Patients With Treatment-Resistant Depressive Episodes in Unipolar and Bipolar Depression. *American Journal of Psychiatry*, *173*(2), 107–111. https://doi.org/10.1176/appi.ajp.2015.15060788

Fox, M. D., & Raichle, M. E. (2007). Spontaneous fluctuations in brain activity observed with functional magnetic resonance imaging. *Nature Reviews Neuroscience*, *8*(9), 700–711. https://doi.org/10.1038/nrn2201

Fox, M. D., Snyder, A. Z., Vincent, J. L., Corbetta, M., Van Essen, D. C., & Raichle, M. E. (2005). The human brain is intrinsically organized into dynamic, anticorrelated functional networks. *Proceedings of the National Academy of Sciences*, *102*(27), 9673–9678. https://doi.org/10.1073/pnas.0504136102

Fox, M. D., Zhang, D., Snyder, A. Z., & Raichle, M. E. (2009). The Global Signal and Observed Anticorrelated Resting State Brain Networks. *Journal of Neurophysiology*, *101*(6), 3270–3283. https://doi.org/10.1152/jn.90777.2008

Frazier, J. A., Chiu, S., Breeze, J. L., Makris, N., Lange, N., Kennedy, D. N., Herbert, M. R., Bent, E. K., Koneru, V. K., Dieterich, M. E., Hodge, S. M., Rauch, S. L., Grant, P. E., Cohen, B. M., Seidman, L. J., Caviness, V. S., & Biederman, J. (2005). Structural Brain Magnetic Resonance Imaging of Limbic and Thalamic Volumes in Pediatric Bipolar Disorder. *American Journal of Psychiatry*, *162*(7), 1256–1265. https://doi.org/10.1176/appi.ajp.162.7.1256

Gabbay, V., Ely, B. A., Li, Q., Bangaru, S. D., Panzer, A. M., Alonso, C. M., Castellanos, F. X., & Milham, M. P. (2013). Striatum-Based Circuitry of Adolescent Depression and Anhedonia. *Journal of the American Academy of Child & Adolescent Psychiatry*, *52*(6), 628-641.e13. https://doi.org/10.1016/j.jaac.2013.04.003

Goldstein, J. M., Seidman, L. J., Makris, N., Ahern, T., O'Brien, L. M., Caviness, V. S., Kennedy, D. N., Faraone, S. V., & Tsuang, M. T. (2007). Hypothalamic Abnormalities in Schizophrenia: Sex Effects and Genetic Vulnerability. *Biological Psychiatry*, *61*(8), 935–945. https://doi.org/10.1016/j.biopsych.2006.06.027

Gorwood, P. (2008). Neurobiological mechanisms of anhedonia. *Dialogues in Clinical Neuroscience*, *10*(3), 291–299. https://doi.org/10.31887/DCNS.2008.10.3/pgorwood

Han, H., Glenn, A. L., & Dawson, K. J. (2019). Evaluating Alternative Correction Methods for Multiple Comparison in Functional Neuroimaging Research. *Brain Sciences*, *9*(8), 198. https://doi.org/10.3390/brainsci9080198

Hauser, T. U., Eldar, E., & Dolan, R. J. (2017). Separate mesocortical and mesolimbic pathways encode effort and reward learning signals. *Proceedings of the National Academy of Sciences*, *114*(35), E7395–E7404. https://doi.org/10.1073/pnas.1705643114

Heidbreder, C. A., Gardner, E. L., Xi, Z.-X., Thanos, P. K., Mugnaini, M., Hagan, J. J., & Ashby, C. R. (2005). The role of central dopamine D3 receptors in drug addiction: a review of pharmacological evidence. *Brain Research Reviews*, *49*(1), 77–105. https://doi.org/10.1016/j.brainresrev.2004.12.033

Heshmati, M., & Russo, S. J. (2015). Anhedonia and the Brain Reward Circuitry in Depression. *Current Behavioral Neuroscience Reports*, *2*(3), 146–153. https://doi.org/10.1007/s40473-015-0044-3

Höflich, A., Michenthaler, P., Kasper, S., & Lanzenberger, R. (2019). Circuit Mechanisms of Reward, Anhedonia, and Depression. *International Journal of Neuropsychopharmacology*, *22*(2), 105–118. https://doi.org/10.1093/ijnp/pyy081

Hu, Y., Zhao, C., Zhao, H., & Qiao, J. (2023). Abnormal functional connectivity of the nucleus accumbens subregions mediates the association between anhedonia and major depressive disorder. *BMC Psychiatry*, *23*(1), 282. https://doi.org/10.1186/s12888-023-04693-0

Hubble, J. P. (2000). Pre-clinical studies of pramipexole: clinical relevance. *European Journal of Neurology*, *7*(SUPPL.1), 15–20. https://doi.org/10.1046/j.1468-1331.2000.0070s1015.x

Jenkinson, M. Chappell, M. (2018). *Introduction to Neuroimaging Analysis*. Oxford University Press.

Jiang, D.-Q., Jiang, L.-L., Wang, Y., & Li, M.-X. (2021). The role of pramipexole in the treatment of patients with depression and Parkinson's disease: A meta-analysis of randomized controlled trials. *Asian Journal of Psychiatry*, *61*, 102691. https://doi.org/10.1016/j.ajp.2021.102691

Jonasson, L. S., Axelsson, J., Riklund, K., Braver, T. S., Ögren, M., Bäckman, L., & Nyberg, L. (2014). Dopamine release in nucleus accumbens during rewarded task switching measured by [11C]raclopride. *NeuroImage*, *99*, 357–364. https://doi.org/10.1016/j.neuroimage.2014.05.047

Joyce, J., & Millan, M. (2007). Dopamine D3 receptor agonists for protection and repair in Parkinson's disease. *Current Opinion in Pharmacology*, *7*(1), 100–105. https://doi.org/10.1016/j.coph.2006.11.004

Jung, J., Kang, J., Won, E., Nam, K., Lee, M.-S., Tae, W. S., & Ham, B.-J. (2014). Impact of lingual gyrus volume on antidepressant response and neurocognitive functions in Major Depressive

Disorder: A voxel-based morphometry study. *Journal of Affective Disorders*, *169*, 179–187. https://doi.org/10.1016/j.jad.2014.08.018

Kane, N., Acharya, J., Beniczky, S., Caboclo, L., Finnigan, S., Kaplan, P. W., Shibasaki, H., Pressler, R., & van Putten, M. J. A. M. (2017). A revised glossary of terms most commonly used by clinical electroencephalographers and updated proposal for the report format of the EEG findings. Revision 2017. *Clinical Neurophysiology Practice*, *2*, 170–185. https://doi.org/10.1016/j.cnp.2017.07.002

Knutson, B., Westdorp, A., Kaiser, E., & Hommer, D. (2000). FMRI Visualization of Brain Activity during a Monetary Incentive Delay Task. *NeuroImage*, *12*(1), 20–27. https://doi.org/10.1006/nimg.2000.0593

Krupp, L. B. (1989). The Fatigue Severity Scale. *Archives of Neurology*, *46*(10), 1121. https://doi.org/10.1001/archneur.1989.00520460115022

Leggio, G. M., Salomone, S., Bucolo, C., Platania, C., Micale, V., Caraci, F., & Drago, F. (2013). Dopamine D3 receptor as a new pharmacological target for the treatment of depression. In *European Journal of Pharmacology,* *719*(1-3), 25-33. https://doi.org/10.1016/j.ejphar.2013.07.022

Li, T., Zou, S., Zhang, Z., Liu, M., & Liang, Z. (2022). Efficacy of pramipexole on quality of life in patients with Parkinson's disease: a systematic review and meta-analysis. *BMC Neurology*, *22*(1), 320. https://doi.org/10.1186/s12883-022-02830-y

Lieberman, M. D., & Cunningham, W. A. (2009). Type I and Type II error concerns in fMRI research: re-balancing the scale. *Social Cognitive and Affective Neuroscience*, *4*(4), 423–428. https://doi.org/10.1093/scan/nsp052

Liu, R., Wang, Y., Chen, X., Zhang, Z., Xiao, L., & Zhou, Y. (2021). Anhedonia correlates with functional connectivity of the nucleus accumbens subregions in patients with major depressive disorder. *NeuroImage: Clinical*, *30*, 102599. https://doi.org/10.1016/j.nicl.2021.102599

Liu, X., Chen, W., Hou, H., Chen, X., Zhang, J., Liu, J., Guo, Z., & Bai, G. (2017). Decreased functional connectivity between the dorsal anterior cingulate cortex and lingual gyrus in Alzheimer's disease patients with depression. *Behavioural Brain Research*, *326*, 132–138. https://doi.org/10.1016/j.bbr.2017.01.037

Lowe, M. J., Mock, B. J., & Sorenson, J. A. (1998). Functional Connectivity in Single and Multislice Echoplanar Imaging Using Resting-State Fluctuations. *NeuroImage*, *7*(2), 119–132. https://doi.org/10.1006/nimg.1997.0315

Luo, Q., Chen, J., Li, Y., Wu, Z., Lin, X., Yao, J., Yu, H., Peng, H., & Wu, H. (2022). Altered regional brain activity and functional connectivity patterns in major depressive disorder: A

function of childhood trauma or diagnosis? *Journal of Psychiatric Research*, *147*, 237–247. https://doi.org/10.1016/j.jpsychires.2022.01.038

Maj, J., Rogói, Z., Margas, W., Kata, M., & Dziedzicka-Wasylewska, M. (2000). The effect of repeated treatment with pramipexole on the central dopamine D3 system. *Journal of Neural Transmission (Vienna, Austria : 1996)*, *107*(12), 1369–1379. https://doi.org/10.1007/s007020070001

Makris, N., Goldstein, J. M., Kennedy, D., Hodge, S. M., Caviness, V. S., Faraone, S. V., Tsuang, M. T., & Seidman, L. J. (2006). Decreased volume of left and total anterior insular lobule in schizophrenia. *Schizophrenia Research*, *83*(2–3), 155–171. https://doi.org/10.1016/j.schres.2005.11.020

Marin, R. S., Biedrzycki, R. C., & Firinciogullari, S. (1991). Reliability and validity of the apathy evaluation scale. *Psychiatry Research*, *38*(2), 143–162. https://doi.org/10.1016/0165-1781(91)90040-V

Martinez-Gutierrez, E., Jimenez-Marin, A., Stramaglia, S., & Cortes, J. M. (2022). The structure of anticorrelated networks in the human brain. *Frontiers in Network Physiology*, *2*. https://doi.org/10.3389/fnetp.2022.946380

McMakin, D. L., Olino, T. M., Porta, G., Dietz, L. J., Emslie, G., Clarke, G., Wagner, K. D., Asarnow, J. R., Ryan, N. D., Birmaher, B., Shamseddeen, W., Mayes, T., Kennard, B., Spirito, A., Keller, M., Lynch, F. L., Dickerson, J. F., & Brent, D. A. (2012). Anhedonia Predicts Poorer Recovery Among Youth With Selective Serotonin Reuptake Inhibitor Treatment–Resistant Depression. *Journal of the American Academy of Child & Adolescent Psychiatry*, *51*(4), 404–411. https://doi.org/10.1016/j.jaac.2012.01.011

Montgomery, S. A., & Åsberg, M. (1979). A New Depression Scale Designed to be Sensitive to Change. *British Journal of Psychiatry*, *134*(4), 382–389. https://doi.org/10.1192/bjp.134.4.382

Morin, C. M., Belleville, G., Bélanger, L., & Ivers, H. (2011). The Insomnia Severity Index: Psychometric Indicators to Detect Insomnia Cases and Evaluate Treatment Response. *Sleep*, *34*(5), 601–608. https://doi.org/10.1093/sleep/34.5.601

Murphy, K., Birn, R. M., Handwerker, D. A., Jones, T. B., & Bandettini, P. A. (2009). The impact of global signal regression on resting state correlations: Are anti-correlated networks introduced? *NeuroImage*, *44*(3), 893–905. https://doi.org/10.1016/j.neuroimage.2008.09.036

Nestler, E. J., & Carlezon, W. A. (2006). The Mesolimbic Dopamine Reward Circuit in Depression. *Biological Psychiatry*, *59*(12), 1151–1159. https://doi.org/10.1016/j.biopsych.2005.09.018

Newson, J. J., & Thiagarajan, T. C. (2019). EEG Frequency Bands in Psychiatric Disorders: A Review of Resting State Studies. *Frontiers in Human Neuroscience*, *12*. https://doi.org/10.3389/fnhum.2018.00521

Nieto-Castanon, A. (2020). *Handbook of functional connectivity Magnetic Resonance Imaging methods in CONN*. Hilbert Press. https://doi.org/10.56441/hilbertpress.2207.6598

Ogawa, S., Lee, T. M., Kay, A. R., & Tank, D. W. (1990). Brain magnetic resonance imaging with contrast dependent on blood oxygenation. *Proceedings of the National Academy of Sciences*, *87*(24), 9868–9872. https://doi.org/10.1073/pnas.87.24.9868

Palejwala, A. H., Dadario, N. B., Young, I. M., O'Connor, K., Briggs, R. G., Conner, A. K., O'Donoghue, D. L., & Sughrue, M. E. (2021). Anatomy and White Matter Connections of the Lingual Gyrus and Cuneus. *World Neurosurgery*, *151*, e426–e437. https://doi.org/10.1016/j.wneu.2021.04.050

Parker, D. B., & Razlighi, Q. R. (2019). The Benefit of Slice Timing Correction in Common fMRI Preprocessing Pipelines. *Frontiers in Neuroscience*, *13*(JUL). https://doi.org/10.3389/fnins.2019.00821

Pizzagalli, D. A. (2022). Toward a Better Understanding of the Mechanisms and Pathophysiology of Anhedonia: Are We Ready for Translation? *American Journal of Psychiatry*, *179*(7), 458–469. https://doi.org/10.1176/appi.ajp.20220423

Pizzagalli, D. A., Holmes, A. J., Dillon, D. G., Goetz, E. L., Birk, J. L., Bogdan, R., Dougherty, D. D., Iosifescu, D. V., Rauch, S. L., & Fava, M. (2009). Reduced Caudate and Nucleus Accumbens Response to Rewards in Unmedicated Individuals With Major Depressive Disorder. *American Journal of Psychiatry*, *166*(6), 702–710. https://doi.org/10.1176/appi.ajp.2008.08081201

Pizzagalli, D. A., Jahn, A. L., & O'Shea, J. P. (2005). Toward an objective characterization of an anhedonic phenotype: A signal-detection approach. *Biological Psychiatry*, *57*(4), 319–327. https://doi.org/10.1016/j.biopsych.2004.11.026

Power, J. D., Barnes, K. A., Snyder, A. Z., Schlaggar, B. L., & Petersen, S. E. (2012). Spurious but systematic correlations in functional connectivity MRI networks arise from subject motion. *NeuroImage*, *59*(3), 2142–2154. https://doi.org/10.1016/j.neuroimage.2011.10.018

Raichle, M. E. (2010). Two views of brain function. *Trends in Cognitive Sciences*, *14*(4), 180–190. https://doi.org/10.1016/j.tics.2010.01.008

Rizvi, S. J., Quilty, L. C., Sproule, B. A., Cyriac, A., Michael Bagby, R., & Kennedy, S. H. (2015). Development and validation of the Dimensional Anhedonia Rating Scale (DARS) in a

community sample and individuals with major depression. *Psychiatry Research*, *229*(1–2), 109–119. https://doi.org/10.1016/j.psychres.2015.07.062

Russo, S. J., & Nestler, E. J. (2013). The brain reward circuitry in mood disorders. *Nature Reviews Neuroscience*, *14*(9), 609–625. https://doi.org/10.1038/nrn3381

Saad, Z. S., Gotts, S. J., Murphy, K., Chen, G., Jo, H. J., Martin, A., & Cox, R. W. (2012). Trouble at Rest: How Correlation Patterns and Group Differences Become Distorted After Global Signal Regression. *Brain Connectivity*, *2*(1), 25–32. https://doi.org/10.1089/brain.2012.0080

Shehzad, Z., Kelly, A. M. C., Reiss, P. T., Gee, D. G., Gotimer, K., Uddin, L. Q., Lee, S. H., Margulies, D. S., Roy, A. K., Biswal, B. B., Petkova, E., Castellanos, F. X., & Milham, M. P. (2009). The Resting Brain: Unconstrained yet Reliable. *Cerebral Cortex*, *19*(10), 2209–2229. https://doi.org/10.1093/cercor/bhn256

Snaith, R. P., Hamilton, M., Morley, S., Humayan, A., Hargreaves, D., & Trigwell, P. (1995). A Scale for the Assessment of Hedonic Tone the Snaith–Hamilton Pleasure Scale. *British Journal of Psychiatry*, *167*(1), 99–103. https://doi.org/10.1192/bjp.167.1.99

Sokoloff, P., & Le Foll, B. (2017). The dopamine D3 receptor, a quarter century later. *European Journal of Neuroscience*, *45*(1), 2–19. https://doi.org/10.1111/ejn.13390

Spijker, J., de Graaf, R., ten Have, M., Nolen, W. A., & Speckens, A. (2010). Predictors of suicidality in depressive spectrum disorders in the general population: results of the Netherlands Mental Health Survey and Incidence Study. *Social Psychiatry and Psychiatric Epidemiology*, *45*(5), 513–521. https://doi.org/10.1007/s00127-009-0093-6

Treadway, M. T., & Zald, D. H. (2011). Reconsidering anhedonia in depression: Lessons from translational neuroscience. *Neuroscience & Biobehavioral Reviews*, *35*(3), 537–555. https://doi.org/10.1016/j.neubiorev.2010.06.006

Trøstheim, M., Eikemo, M., Meir, R., Hansen, I., Paul, E., Kroll, S. L., Garland, E. L., & Leknes, S. (2020). Assessment of Anhedonia in Adults With and Without Mental Illness. *JAMA Network Open*, *3*(8), e2013233. https://doi.org/10.1001/jamanetworkopen.2020.13233

Tundo, A., Betro', S., Iommi, M., & de Filippis, R. (2022). Efficacy and safety of 24-week pramipexole augmentation in patients with treatment resistant depression. A retrospective cohort study. *Progress in Neuro-Psychopharmacology and Biological Psychiatry*, *112*, 110425. https://doi.org/10.1016/j.pnpbp.2021.110425

Tundo, A., Filippis, R., & De Crescenzo, F. (2019). Pramipexole in the treatment of unipolar and bipolar depression. A systematic review and meta-analysis. *Acta Psychiatrica Scandinavica*, *140*(2), 116–125. https://doi.org/10.1111/acps.13055

Veer, I. M. (2010). Whole brain resting-state analysis reveals decreased functional connectivity in major depression. *Frontiers in Systems Neuroscience*, *4*. https://doi.org/10.3389/fnsys.2010.00041

Ventorp, F., Lindahl, J., van Westen, D., Jensen, J., Björkstrand, J., & Lindqvist, D. (2022). Preliminary Evidence of Efficacy and Target Engagement of Pramipexole in Anhedonic Depression. *Psychiatric Research and Clinical Practice*, *4*(2), 42–47. https://doi.org/10.1176/appi.prcp.20210042

Vrieze, E., Pizzagalli, D. A., Demyttenaere, K., Hompes, T., Sienaert, P., de Boer, P., Schmidt, M., & Claes, S. (2013). Reduced Reward Learning Predicts Outcome in Major Depressive Disorder. *Biological Psychiatry*, *73*(7), 639–645. https://doi.org/10.1016/j.biopsych.2012.10.014

Wacker, J., Dillon, D. G., & Pizzagalli, D. A. (2009). The role of the nucleus accumbens and rostral anterior cingulate cortex in anhedonia: Integration of resting EEG, fMRI, and volumetric techniques. *NeuroImage*, *46*(1), 327–337. https://doi.org/10.1016/j.neuroimage.2009.01.058

Wang, G.-J., Volkow, N. D., & Fowler, J. S. (2002). The role of dopamine in motivation for food in humans: implications for obesity. *Expert Opinion on Therapeutic Targets*, *6*(5), 601–609. https://doi.org/10.1517/14728222.6.5.601

Weiler, M., Casseb, R. F., de Campos, B. M., Crone, J. S., Lutkenhoff, E. S., Vespa, P. M., & Monti, M. M. (2022). Evaluating denoising strategies in resting-state functional magnetic resonance in traumatic brain injury (EpiBioS4Rx). *Human Brain Mapping*, *43*(15), 4640–4649. https://doi.org/10.1002/hbm.25979

Weintraub, D., Mamikonyan, E., Papay, K., Shea, J. A., Xie, S. X., & Siderowf, A. (2012). Questionnaire for impulsive-compulsive disorders in Parkinson's Disease-Rating Scale. *Movement Disorders*, *27*(2), 242–247. https://doi.org/10.1002/mds.24023

Whitfield-Gabrieli, S., & Nieto-Castanon, A. (2012). *Conn* : A Functional Connectivity Toolbox for Correlated and Anticorrelated Brain Networks. *Brain Connectivity*, *2*(3), 125–141. https://doi.org/10.1089/brain.2012.0073

Wilson, R. P., Colizzi, M., Bossong, M. G., Allen, P., Kempton, M., & Bhattacharyya, S. (2018). The Neural Substrate of Reward Anticipation in Health: A Meta-Analysis of fMRI Findings in the Monetary Incentive Delay Task. *Neuropsychology Review*, *28*(4), 496–506. https://doi.org/10.1007/s11065-018-9385-5

Woo, C.-W., Krishnan, A., & Wager, T. D. (2014). Cluster-extent based thresholding in fMRI analyses: Pitfalls and recommendations. *NeuroImage*, *91*, 412–419. https://doi.org/10.1016/j.neuroimage.2013.12.058

World Medical Association Declaration of Helsinki. (2013). *JAMA*, *310*(20), 2191. https://doi.org/10.1001/jama.2013.281053

Xia, X., Fan, L., Cheng, C., Eickhoff, S. B., Chen, J., Li, H., & Jiang, T. (2017). Multimodal connectivity-based parcellation reveals a shell-core dichotomy of the human nucleus accumbens. *Human Brain Mapping*, *38*(8), 3878–3898. https://doi.org/10.1002/hbm.23636

Xie, C., Jia, T., Rolls, E. T., Robbins, T. W., Sahakian, B. J., Zhang, J., Liu, Z., Cheng, W., Luo, Q., Zac Lo, C.-Y., Wang, H., Banaschewski, T., Barker, G. J., Bokde, A. L. W., Büchel, C., Quinlan, E. B., Desrivières, S., Flor, H., Grigis, A., … Zhang, Y. (2021). Reward Versus Nonreward Sensitivity of the Medial Versus Lateral Orbitofrontal Cortex Relates to the Severity of Depressive Symptoms. *Biological Psychiatry: Cognitive Neuroscience and Neuroimaging*, *6*(3), 259–269. https://doi.org/10.1016/j.bpsc.2020.08.017

Yager, L. M., Garcia, A. F., Wunsch, A. M., & Ferguson, S. M. (2015). The ins and outs of the striatum: Role in drug addiction. *Neuroscience*, *301*, 529–541. https://doi.org/10.1016/j.neuroscience.2015.06.033

Young, C. B., Chen, T., Nusslock, R., Keller, J., Schatzberg, A. F., & Menon, V. (2016). Anhedonia and general distress show dissociable ventromedial prefrontal cortex connectivity in major depressive disorder. *Translational Psychiatry*, *6*(5), e810–e810. https://doi.org/10.1038/tp.2016.80

Young, M. M., & Wohl, M. J. A. (2011). The Canadian Problem Gambling Index: An Evaluation of the Scale and Its Accompanying Profiler Software in a Clinical Setting. *Journal of Gambling Studies*, *27*(3), 467–485. https://doi.org/10.1007/s10899-010-9224-y

Young, R. C., Biggs, J. T., Ziegler, V. E., & Meyer, D. A. (1978). A Rating Scale for Mania: Reliability, Validity and Sensitivity. *British Journal of Psychiatry*, *133*(5), 429–435. https://doi.org/10.1192/bjp.133.5.429

Zhang, B., Lin, P., Shi, H., Öngür, D., Auerbach, R. P., Wang, X., Yao, S., & Wang, X. (2016). Mapping anhedonia-specific dysfunction in a transdiagnostic approach: an ALE meta-analysis. *Brain Imaging and Behavior*, *10*(3), 920–939. https://doi.org/10.1007/s11682-015-9457-6

Appendix A

Table A1

Significant Clusters of Resting-state Functional Connectivity with the NAc, Pre-treatment

Cluster location		Hemisphere	Peak voxel (MNI) coordinates			Number of voxels	F-value	*P-value* (uncorrected)	*P*-value (FDR)
			X	Y	Z				
Subcallosal cortex, striatum			8	10	-2	3532	116.50	<0.001	<0.001
	Subcallosal cortex	Bilateral	0	16	-10	279			
	Putamen	Right	22	10	-6	261			
	Putamen	Left	-20	10	-2	250			
	Caudate	Right	12	16	2	227			
	Caudate	Left	-12	16	2	257			
	Nucleus Accumbens	Right	10	12	-6	84			
	Nucleus Accumbens	Left	-10	12	-8	107			
	Insular cortex	Right	34	16	-8	97			
	Insular cortex	Left	-32	14	-12	36			
	Frontal orbital cortex	Right	22	18	16	73			
	Frontal orbital cortex	Left	-16	16	-16	79			
	Pallidum	Right	16	4	-4	24			
	Pallidum	Left	-14	4	-2	23			
	Frontal pole	Right	22	36	-14	21			
	Frontal pole	Left	-20	38	-16	2			
	Brain stem	N/A	0	-18	-20	15			
	Thalamus	Left	-6	-2	0	12			
	White matter	N/A	4	12	-4	1685			
Frontal pole/anterior cingulate gyrus			8	42	-6	2530	43.05	<0.001	<0.001
	Frontal pole	Right	10	60	-2	175			
	Frontal pole	Left	-20	60	2	549			
	Anterior cingulate gyrus	Bilateral	0	38	2	386			
	Paracingulate gyrus	Right	6	46	-2	291			
	Paracingulate gyrus	Left	-6	46	-2	273			
	Medial frontal cortex	Bilateral	0	48	-10	242			
	Subcallosal cortex	Bilateral	2	30	-10	12			
	White matter	N/A	0	50	-2	602			
Superior frontal gyrus		Left	-26	32	50	773	35.03	<0.001	<0.001
Frontal pole/paracingulate frontal gyrus		Bilateral	12	40	48	581	71.90	<0.001	<0.001
Precentral gyrus		Left	-26	-18	64	216	16.86	0.002	0.003
Cerebellar vermis/cerebelum		Bilateral	2	-54	-10	158	17.46	0.002	0.003
Inferior temporal gyrus		Right	58	-42	-26	129	19.43	0.001	0.003
Putamen, white matter		Left	-30	-4	-12	91	25.34	<0.001	0.002
Precentral gyrus/posterior cingulate gyrus		Left	-8	-26	50	89	21.35	0.001	0.003
Precuneous		Bilateral	02	-74	46	85	11.55	0.006	0.007
White matter		Right	26	-42	18	80	35.78	<0.001	<0.001
Precentral gyrus, white matter		Right	12	-26	58	72	17.46	0.002	0.003
Superior parietal lobule, white matter		Left	-20	-56	74	67	20.66	0.001	0.003
Planum Temporale		Right	54	-12	0	53	14.97	0.003	0.004
Caudate, white matter		Left	-24	-16	26	47	17.76	0.002	0.003
Supplementary Motor Cortex		Right	4	0	60	42	12.53	0.005	0.006
Supplementary Motor Cortex		Left	-10	-08	54	35	41.89	<0.001	<0.001
Heschl's Gyrus		Left	-40	-26	2	35	9.99	0.009	0.009
Thalamus		Left	-8	-20	10	33	18.04	0.002	0.003
Anterior cingulate gyrus/supplementary motor cortex		Right	10	-4	46	27	8.09	0.015	0.015

Note. Significant clusters of resting state functional connectivity of the NAc ROI (bilateral), pre-treatment main effect. Clusters covering more than 1000 voxels are further subdivided into regions included in the cluster.

Table A2

Significant Clusters of Resting-state Functional Connectivity with the NAc, Post-treatment

Cluster location		Hemisphere	Peak voxel (MNI) coordinates			Number of voxels	F-value	*P-value* (uncorrected)	*P*-value (FDR)
			X	Y	Z				
Anterior cingulate gyrus, striatum			+8	+12	-4	8486	47.09	<0.001	<0.001
	Anterior cingulate gyrus	Bilateral	0	40	6	592			
	Paracingulate gyrus	Right	6	46	2	333			
	Paracingulate gyrus	Left	-6	46	4	480			
	Subcallosal cortex	Bilateral	0	20	-8	370			
	Caudate	Right	12	14	6	315			
	Caudate	Left	-12	14	4	337			
	Medial frontal cortex	Bilateral	0	48	-12	271			
	Putamen	Right	22	10	-4	267			
	Putamen	Left	-20	10	-4	262			
	Frontal pole	Right	26	50	-2	257			
	Frontal pole	Left	-18	56	-4	226			
	Orbital frontal cortex	Right	24	22	-14	224			
	Orbital frontal cortex	Left	-22	22	-16	196			
	Thalamus	Right	6	-12	4	65			
	Thalamus	Left	-6	-12	2	149			
	Nucleus Accumbens	Right	10	12	-6	84			
	Nucleus Accumbens	Left	-10	12	-8	107			
	Insular cortex	Right	32	16	-8	100			
	Insular cortex	Left	-34	12	-8	88			
	Pallidum	Right	16	4	-2	62			
	Pallidum	Left	-14	4	-2	31			
	Amygdala	Right	14	-8	-14	7			
	Amygdala	Left	-16	-6	-16	23			
	Temporal pole	Left	-32	6	-20	22			
	White matter	Bilateral	4	20	-2	3618			
Superior lateral occipital cortex, white matter		Left	-32	-66	+24	235	24.54	<0.001	0.002
Central opercular cortex, white matter		Left	-34	-10	-10	197	40.01	<0.001	<0.001
Frontal pole		Right	+34	+44	+40	137	18.23	0.002	0.002
Planum Polare, white matter		Right	+48	-14	-4	95	14.07	0.004	0.004
Precentral gyrus		Left	-18	-32	+62	90	20.84	0.001	0.002
Precentral gyrus		Right	+18	-26	+58	80	14.56	0.003	0.004
Supplementary motor cortex/white matter		Right	+14	-06	+58	77	27.66	<0.001	0.001
Frontal pole		Left	-12	+46	+42	67	16.21	0.002	0.003
Cerebellar vermis/cerebellum		Bilateral	-4	-52	-16	57	18.87	0.002	0.002
Postcentral gyrus		Right	+48	-28	+62	56	10.27	0.008	0.008
White matter		Right	+26	-34	+28	56	68.83	<0.001	<0.001
Temporal pole		Left	-56	+06	-28	51	17.35	0.002	0.003
Inferior lateral occipital cortex		Right	+52	-78	+10	49	18.42	0.002	0.002
White matter		Left	-26	+14	+30	39	20.97	0.001	0.002
Superior parietal lobule, white matter		Right	+26	-50	+46	36	33.58	<0.001	<0.001
White matter		Right	+28	-56	+16	34	33.94	<0.001	<0.001

Note. Significant clusters of resting state functional connectivity of the NAc ROI (bilateral), post-treatment main effect. Clusters covering more than 1000 voxels are further subdivided into regions included in the cluster.